Conf-910836--1

Fermi National Accelerator Laboratory

FNAL/C--91/273

DE92 002674

RECEIVED by OSTI

NOV 12 1991

Recent Results from the E665 Muon Scattering Experiment at Fermilab

The Fermilab E665 Collaboration

presented by H. E. Montgomery

Fermi National Accelerator Laboratory
P.O. Box 500, Batavia, Illinois 60510

DISCLAIMER

This report was prepared as an account of work sponsored by an agency of the United States Government. Neither the United States Government nor any agency thereof, nor any of their employees, makes any warranty, express or implied, or assumes any legal liability or responsibility for the accuracy, completeness, or usefulness of any information, apparatus, product, or process disclosed, or represents that its use would not infringe privately owned rights. Reference herein to any specific commercial product, process, or service by trade name, trademark, manufacturer, or otherwise does not necessarily constitute or imply its endorsement, recommendation, or favoring by the United States Government or any agency thereof. The views and opinions of authors expressed herein do not necessarily state or reflect those of the United States Government or any agency thereof.

October 1991

* Presented at the *Topical Conference of the SLAC Summer Institute*, SLAC, August 1991.

MASTER

DISTRIBUTION OF THIS DOCUMENT IS UNLIMITED

Operated by Universities Research Association Inc. under contract with the United States Department of Energy

Recent Results from the E665 Muon Scattering Experiment at Fermilab

THE FERMILAB E665 COLLABORATION

October 5, 1991

Abstract

Recent results from the high energy muon scattering experiment, E665 at Fermilab are presented. In particular we discuss results on the ratio of cross-sections measured using Xenon and Deuterium at exceptionally low x_{Bj}, the x_{Bj} lower limit is approximately two orders of magnitude lower than any leptoproduction results previously reported. Neutron-proton ratio measurements are discussed in terms of the Gottfried Sum Rule and a measurement of the low x_{Bj} contribution to the Gottfried Sum is presented. Forward fragmentation in muon scattering is compared to fragmentation as observed in other processes. Finally we discuss measurements of the rates of production of forward multi-jet topologies.

Presented by H.E.Montgomery, Fermi National Accelerator Laboratory

THE FERMILAB E665 COLLABORATION

M. R. Adams[6], S. Aïd[9], P. L. Anthony[10,a], M. D. Baker[10], J. Bartlett[4], A. A. Bhatti[13,b], H. M. Braun[14], W. Busza[10], J. M. Conrad[5], G. Coutrakon[4,c], R. Davisson[13], I. Derado[11], S. K. Dhawan[15], W. Dougherty[13], T. Dreyer[1], K. Dziunikowska[8], V. Eckardt[11], U. Ecker[14], M. Erdmann[1,e], A. Eskreys[7], J. Figiel[7], H. J. Gebauer[11], D. F. Geesaman[2], R. Gilman[2,d], M. C. Green[2,f], J. Haas[1], C. Halliwell[6], J. Hanlon[4], D. Hantke[11], V. W. Hughes[15], H. E. Jackson[2], D. E. Jaffe[6], G. Jancso[11], D. M. Jansen[13], S. Kaufman[2], R. D. Kennedy[3], T. Kirk[4,g], H. G. E. Kobrak[3], S. Krzywdzinski[4], S. Kunori[9], J. J. Lord[13], H. J. Lubatti[13], D. McLeod[6], S. Magill[6,g], P. Malecki[7], A. Manz[11], H. Melanson[4], D. G. Michael[5,h], W. Mohr[1], H. E. Montgomery[4], J. G. Morfin[4], R. B. Nickerson[5,i], S. O'Day[9,j], K. Olkiewicz[7], L. Osborne[10], V. Papavassiliou[15,g], B. Pawlik[7], F. M. Pipkin[5], E. J. Ramberg[9,j], A. Röser[14,k], J. J. Ryan[10], C. Salgado[4], A. Salvarani[3,k], H. Schellman[12], M. Schmitt[5], N. Schmitz[11], K. P. Schüler[15], H. J. Seyerlein[11], A. Skuja[9], G. A. Snow[9], S. Söldner-Rembold[11], P. H. Steinberg[9,l], H. E. Stier[1,l], P. Stopa[7], R. A. Swanson[3], R. Talaga[9,g], S. Tentindo-Repond[2,m], H.-J. Trost[2], M. Vidal[11] M. Wilhelm[1], J. Wilkes[13], H. Venkataramania[15], Richard Wilson[5], W. Wittek[11], S. A. Wolbers[4], T. Zhao[13]

[1] Albert-Ludwigs-Universität Freiburg i. Br., Germany
[2] Argonne National Laboratory, Argonne IL USA
[3] University of California, San Diego, CA USA
[4] Fermi National Accelerator Laboratory, Batavia, IL US A
[5] Harvard University, Cambridge, MA USA
[6] University of Illinois, Chicago, IL USA
[7] Institute for Nuclear Physics, Krakow, Poland
[8] Institute for Nuclear Physics, Academy of Mining and Metallurgy, Krakow, Poland
[9] University of Maryland, College Park, MD USA
[10] Massachusetts Institute of Technology, Cambridge, M A USA
[11] Max-Planck-Institute, Munich, Germany
[12] Northwestern University, Evanston, IL USA
[13] University of Washington, Seattle, WA USA
[14] University of Wuppertal, Wuppertal, Germany
[15] Yale University, New Haven, CT USA

Introduction

For experiment E665 at Fermilab, the 1987-88 fixed target period was the first time that the full apparatus was exposed to beam. This initial phase of the experiment has proved fruitful both in terms of students' Ph. D. theses [1, 2, 3, 4, 5, 6, 7, 8, 9, 10] [11, 12, 13] and in terms of written conference contributions and publications[14, 15, 16, 17] [18, 19, 20, 21] [22, 23, 24]. In this presentation we will select four aspects of the analysis of the data which are proving to be particularly interesting and which, at least in part, represent the newest results from E665. We will not refer to the data taken in 1990 nor to that currently being accumulated.

The kinematic quantities relevant to structure function physics are determined entirely by measurement of the incident and scattered muon. The kinematics of the muon scattering process, described by the exchange of a single virtual photon, for a fixed beam energy E, is defined by two Lorentz invariant variables. Q^2 is the modulus of the square of the virtual photon four-momentum, $\nu = E - E_\mu$ is its energy in the lab system and m_p is the mass of the target nucleon which is assumed to be at rest. x_{Bj} is then given by $x_{Bj} = Q^2/2m_p\nu$. These measures, with the addition of the hadronic centre of mass energy W^2, $W^2 = 2m_p\nu + m_p^2 - Q^2$, also largely characterise the event for hadronic physics. In addition we will utilise other measures for the hadrons which we will define at the appropriate time.

The muon beam [25] is derived by impinging the extracted, 800 GeV proton beam on a Beryllium target. The resultant pions are collected in a system of focussing-defocussing quadrupoles and transported for about a kilometre at which point a few percent of them have decayed to muons. The hadrons are arrested by a long Beryllium absorber and the penetrating muons are transported through a second quadrupole system to the experiment. During this last 300 metres of flight the outlying muons are scraped away using magnetised iron elements, a mu-pipe and a set of toroids, which considerably reduces the rate of halo muons at the experiment. In addition a final 3 mr bend in the beam permits the measurement of momentum and direction of each individual muon.

The experiment [26], depicted in Fig. 1, consists of two large superconducting dipoles and numerous planes of multi-wire drift and proportional chambers. The spectrometer is open and is thus sensitive to the hadronic products of the muon interactions as well as to the scattered leptons. In addition to charged tracks, the forward going neutral pions and photons are detected in an electromagnetic calorimeter. The neutral pions, which decay to two photons, have similar origins to the charged pions. However individual photons may also be produced by radiation from the muons participating in the interaction. They are a part of the *radiative corrections*. In one of the analyses presented below, the calorimeter has been used to identify those events with and without significant radiation from the muon.

Two independent triggers, which were sensitive over different ranges of scattering angle, are relevant to the measurements presented here. The Small Angle Trigger (SAT) used the beam hodoscopes to project a subset of the individual incident muon trajectories to the rear of the apparatus where the absence of an appropriate set of hodoscope hits signalled a scatter. The Large Angle Trigger (LAT) used a similar principle but employed the entire beam envelope as defined by the beam hodoscopes and consequently gained in luminosity at the cost of a larger minimum scattering angle. The acceptances of the two triggers in the $Q^2 - \nu$ plane are shown in Fig. 2. In both cases, the scattered muon was chosen from candidate tracks reconstructed in the open geometry spectrometer by its link to a multi-plane trajectory found downstream of a two metre thick iron absorber. The use of two independent triggers permitted a measurement of trigger efficiency for some of the measurements. The number of incident muons was measured independently for each trigger using cross-checking methods including a random sampling of the beams. This permitted the evaluation of cross-section ratios and will lead eventually to determinations of absolute cross-sections and structure functions.

In all measurements discussed here, reconstruction efficiencies and acceptances were evaluated by extensive Monte Carlo modeling of the individual detector elements and complete reconstruction of the Monte Carlo data.

E665 apparatus

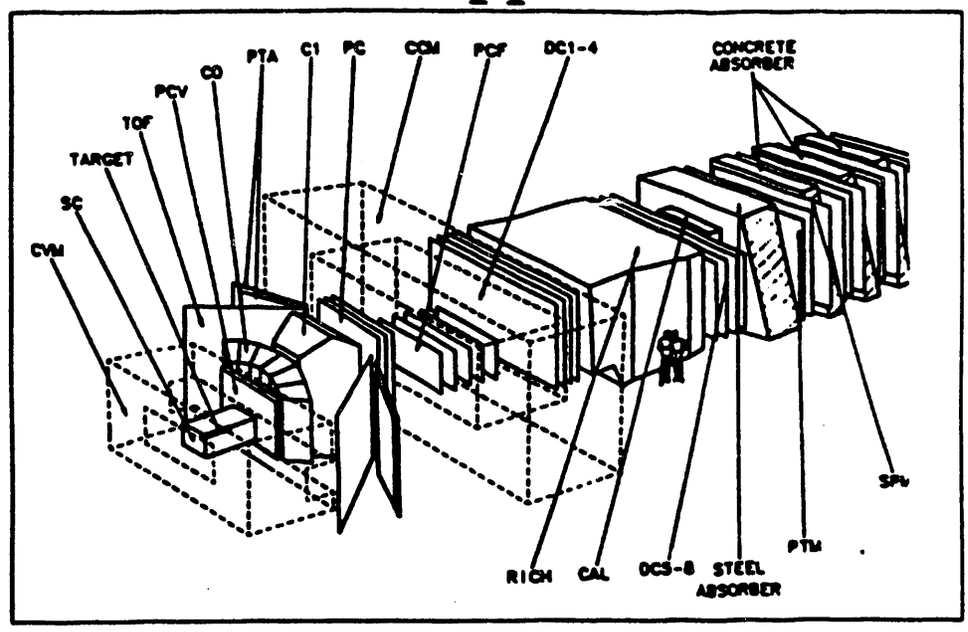

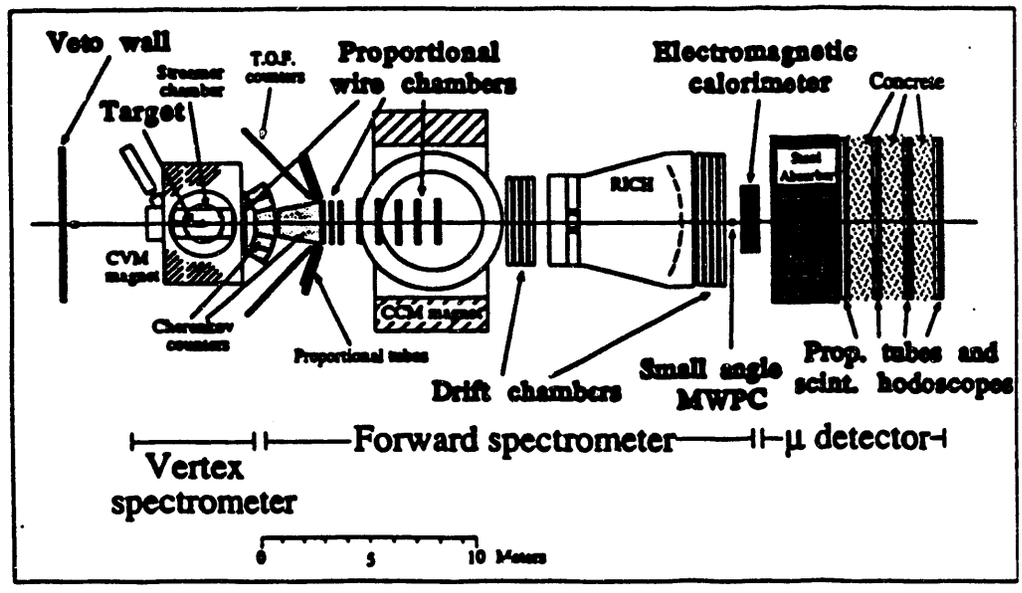

Figure 1
The E665 Apparatus.

Acceptance

Large angle trigger

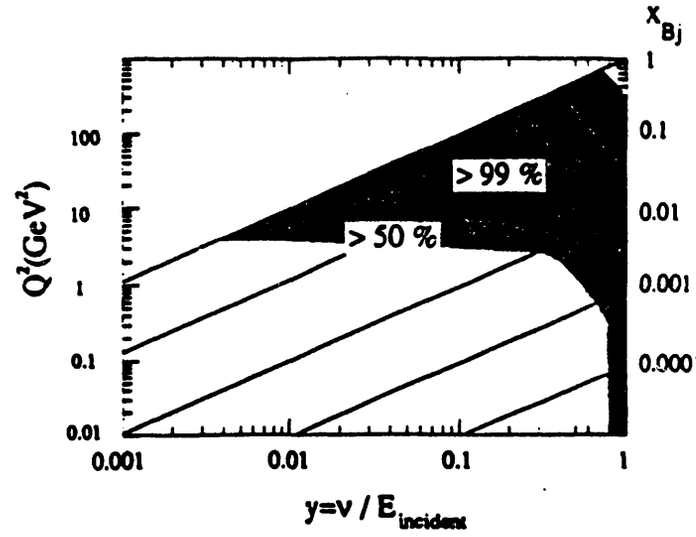

Small angle trigger

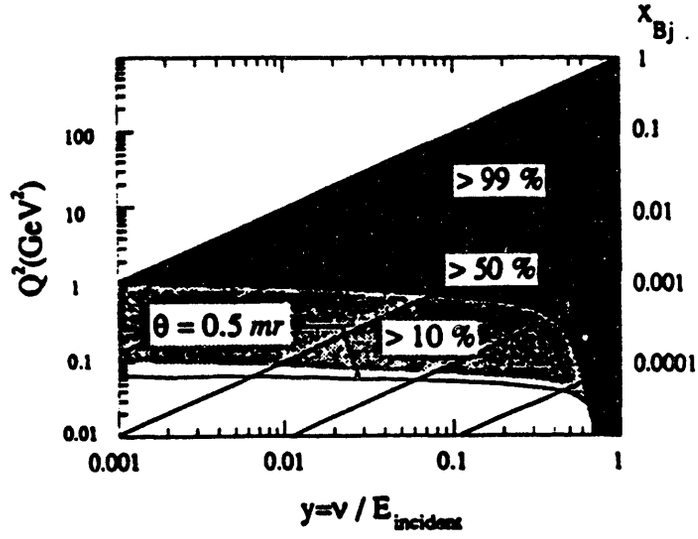

Figure 2
Acceptance in the Q^2-ν plane of the two primary physics triggers.

Xenon/Deuterium Cross-section Ratios at Extremely Low x_{Bj}

Understanding the interactions of photons, real and virtual, with nuclear matter has often taken recourse to measurements of the ratios of cross-sections on various nuclei to those on Deuterium. When a depletion of the *per nucleon* cross-section is observed it is called shadowing although some people associate this term with the low x_{Bj} region only. Until now the lowest x_{Bj}, above photoproduction, for which measurements existed has been $x_{Bj} \simeq 0.001$. Below that value radiative processes and $\mu - e$ scattering become very important.

In Fig. 3a we show the distributions, in the $Q^2 - \nu$ plane, of events from the Xenon target. The general high population at low x_{Bj} is evident for Xenon. In the Deuterium data, Fig. 3b, we are able to clearly see the $\mu - e$ elastic scattering peak which occurs at $x_{Bj} = m_e/m_p$.

A previous analysis [7, 18] resulted in the measurements shown in Fig. 4.The Xenon/Deuterium ratio is compared to similar data from NMC [27] using Calcium and Deuterium. The ratio decreases rather strongly as x_{Bj} decreases and there is no indication of this trend ending. This is surprising since the photoproduction measurements have values of about 0.7 and the measurements with $x_{Bj} \neq 0$, $Q^2 \neq 0$ must extrapolate continuously to the photoproduction point.

The new measurements from E665[22] have attempted to avoid or reduce the radiative effects by explicitly identifying inelastic scatters using the full information on both hadronic tracks and on the calorimeter signals. Two somewhat different approaches have been used and each has been checked against Monte Carlo simulation. The two methods agree in the ratio. The results are shown in Fig. 5. They extend, by two orders of magnitude, the lower limit in x_{Bj}. These data are consistent with the analysis at higher x_{Bj} and with the previous measurements but, importantly, a saturation is clearly seen. The ratio is constant below $x_{Bj} = 0.001$ and is consistent with the estimates derived from photoproduction data.

It would appear that the bridge between virtual and real photons has been made, the data constrain the descriptions of the interactions of photons with matter.

a

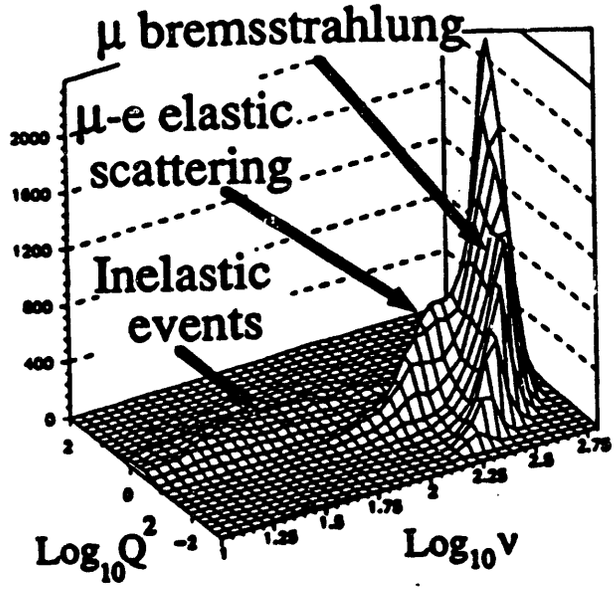

b

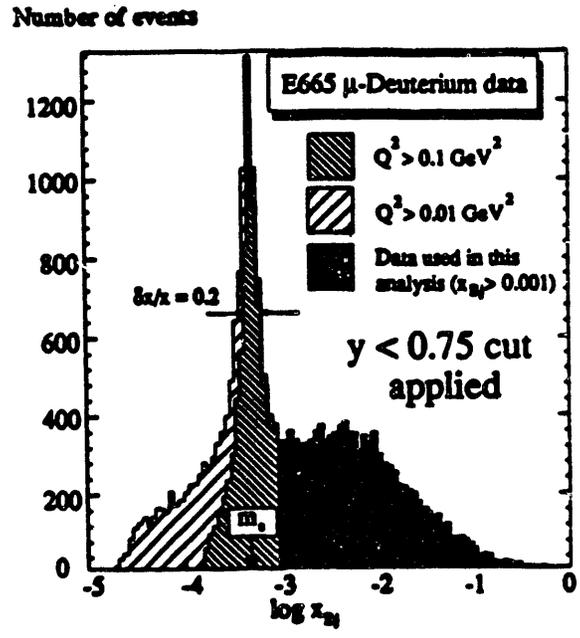

Figure 3

Event distributions: a) versus Q^2 and ν from the xenon target for the SAT trigger, b) versus x_{Bj} for the deuterium target showing the peak from elastic muon electron scattering.

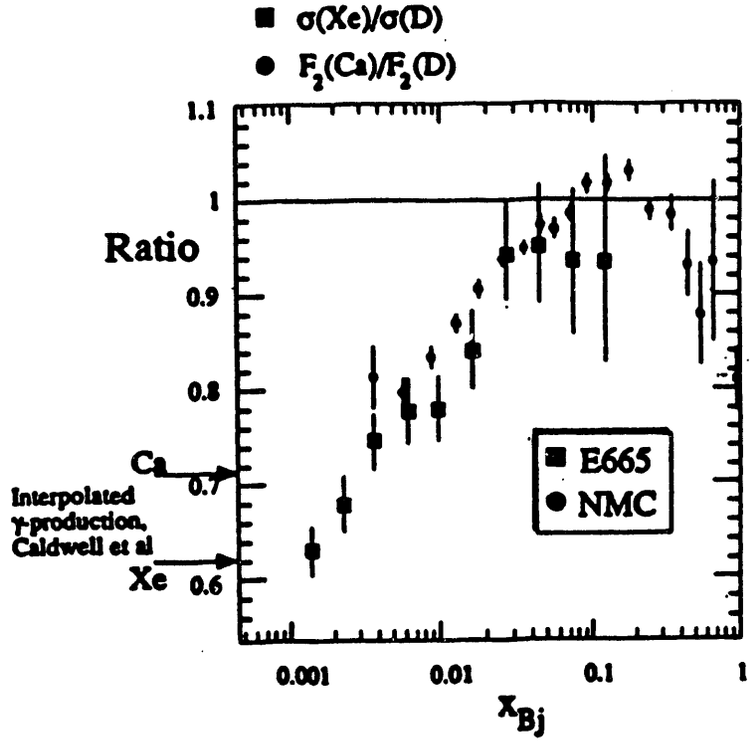

Figure 4

Comparison of E665 data for Xe/D compared to Ca/D from NMC at moderately low x_{Bj}.

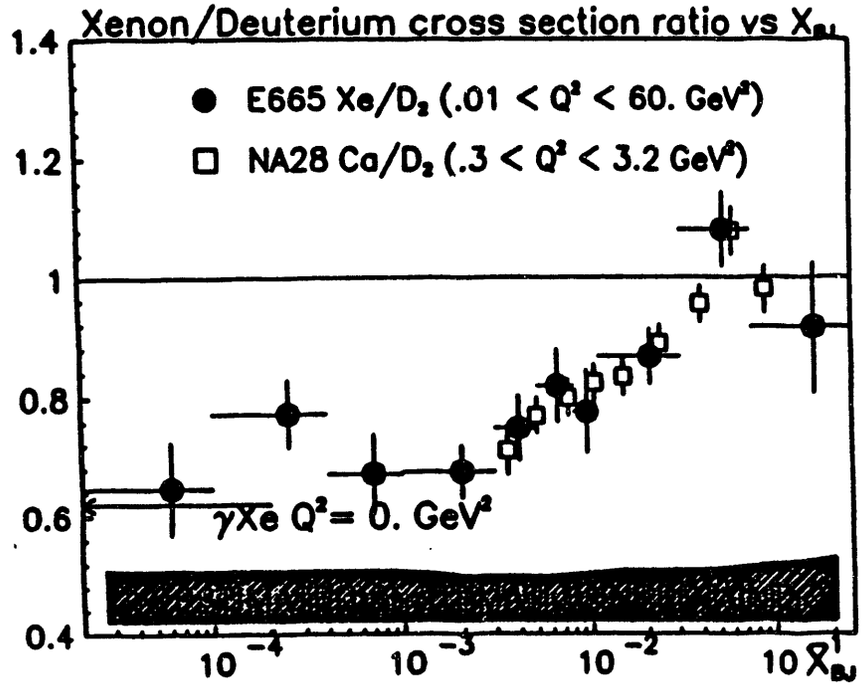

Figure 5

Comparison of E665 data for Xe/D compared to Ca/D from EMC/NA28 at extremely low x_{Bj}, the dark bar indicates the systematic error in the E665 data.

Neutron Proton Cross-section Ratios and the Gottfried Sum Rule

The sensitivity of a measurement of the ratio of, or the difference between, proton and neutron structure functions to the relative fractions of up and down quarks in the nucleon has long been recognized [28]. Further the Gottfried Sum Rule [29, 28] makes the prediction

$$\int_0^1 (F_2^p - F_2^n) \frac{dx_{Bj}}{x_{Bj}} = \frac{1}{3}.$$

The evaluation uses the quark parton model and assumes isospin symmetry of the quark anti-quark sea although deviations have been contemplated[30]. Measurements [31, 32, 33, 34] have been made using both electron and muon beams. In none of these experiments was the sum rule found to be saturated, however each was limited at low x_{Bj} by the range and precision of the data. Recently determinations [35, 36] of the sum have been made which extend the range of the data to somewhat lower x_{Bj} but which still do not find that the sum rule is saturated. The smallness of the statistical and systematic errors has led to much theoretical speculation [37, 38] as to the cause of the discrepancy.

Measurements were made with both Hydrogen and Deuterium targets using the same target vessel and separated in time by about one month. The combination of measurements permits the extraction of the ratios and differences of proton and neutron cross-sections. The preliminary evaluation of the ratio was presented [17] in 1990 and is reproduced in Fig. 6. The errors in this case included the contributions from limited Monte Carlo data on a point to point basis. In the evaluation described below a somewhat different approach has been utilised.

The basic ratios σ_n/σ_p for the SAT data are shown in Fig. 7 with statistical errors only. One should note that the mean Q^2 values vary with x_{Bj} from 0.5 GeV^2 at the lowest x_{Bj} to 16.0 GeV^2 at the highest. Possible corrections due to performance differences in the apparatus (the beam counting, the trigger acceptance and efficiency, the track acceptance and reconstruction efficiency) are all at the level of a few percent or less. In order to gauge their combined effect we have identified and analysed the elastic muon electron scattering process from each target. The signal, a characteristic peak in $x_{Bj} = m_e/m_p$, extracted using the electromagnetic calorimeter to identify electrons is shown in Fig. 8 for each target. With the luminosity corrections included, the relative yield from each is

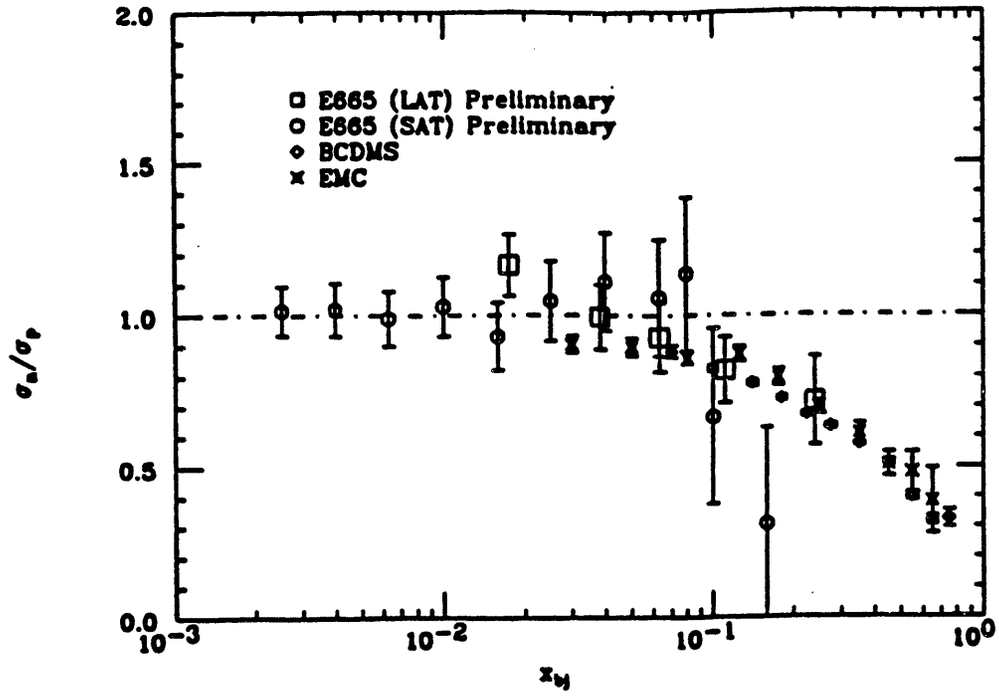

Figure 6
Neutron-proton ratio from E665, preliminary results from 1990.

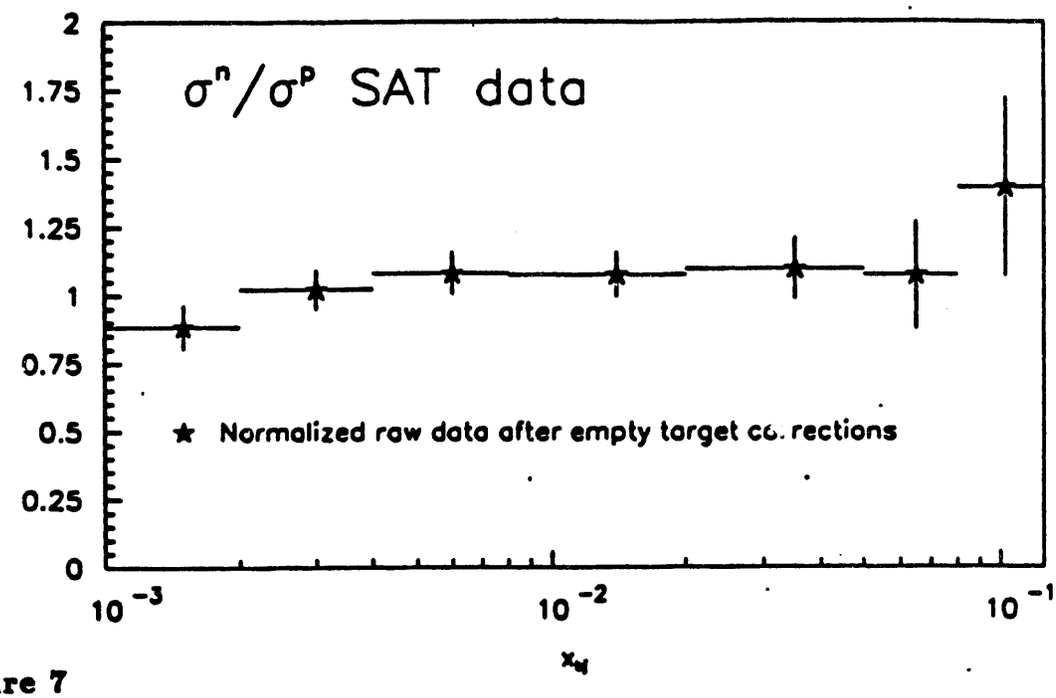

Figure 7
Neutron-proton ratio, data corrected only for relative normalisation and empty target contributions.

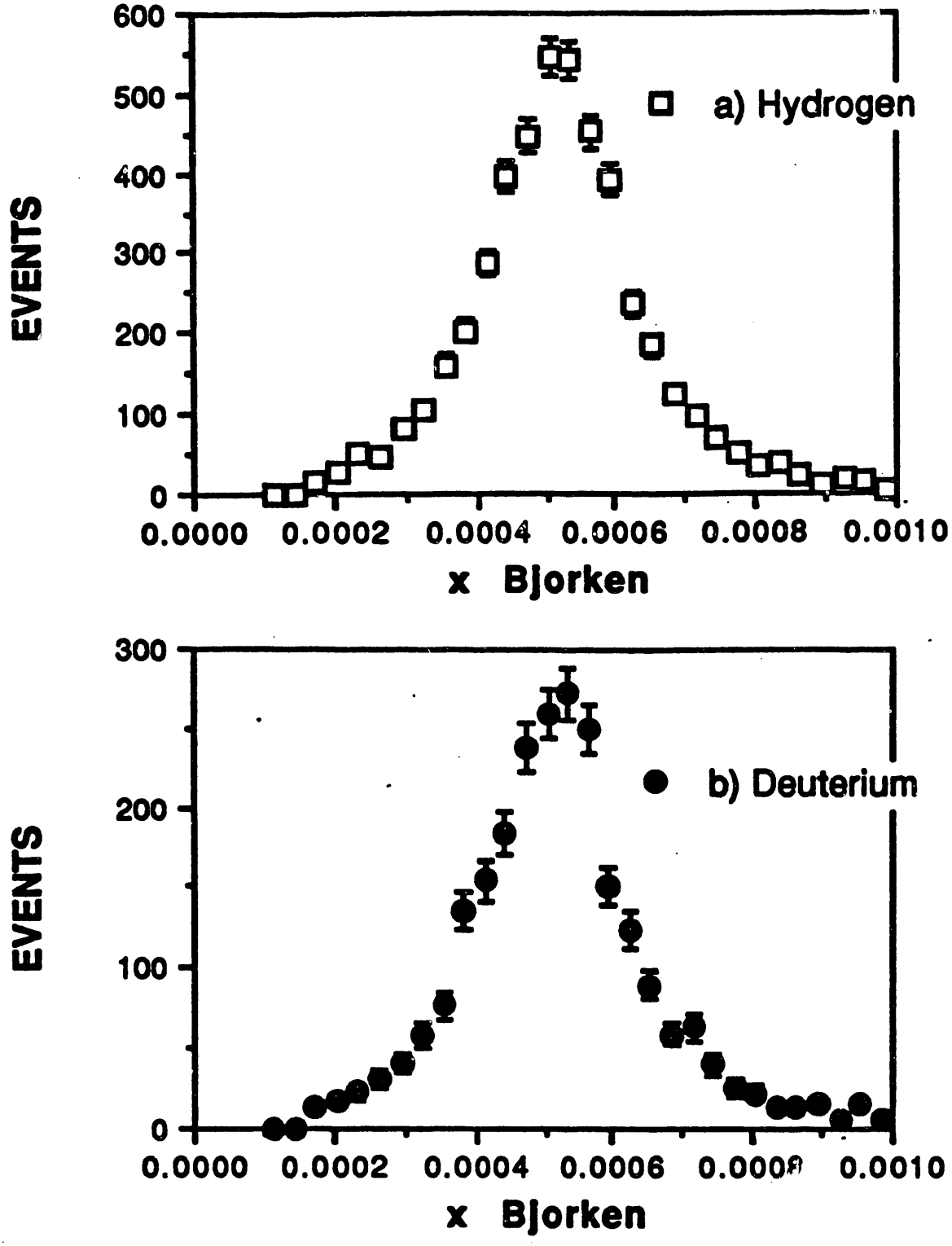

Figure 8
Muon electron scattering yields from a) Hydrogen and b) Deuterium targets.

equal to within a few percent. Consequently we have applied no corrections to the raw data ratios except for the luminosity. This procedure is entirely analogous to the methods used some years ago in low energy electron scattering when numerous measurements of the elastic electron-proton scattering cross-section were included in the cycles of data taking. In most high energy experiments the opportunity, the luxury, of a well defined reference process has been absent. Retrospectively this justifies the efforts made in E665 to retain measurement sensitivity down to zero scattering angle. In principle there are corrections to be made for the binding of the nucleons in the deuteron however these are negligible in this kinematic regime. Radiative corrections have been calculated and very small differences were found between neutrons and protons. These corrections have not been applied.

In order to evaluate the contribution to the Gottfried Sum we proceed as follows. Other experiments [39] have measured the ratio of longitudinal to transverse components of the cross-section to be the same for Hydrogen and Deuterium. This permits us to make the identification $F_2^n/F_2^p=\sigma_n/\sigma_p=r(x_{Bj})$. We then calculate the quantity $F_2^p - F_2^n = 2F_2^d(1-r(x_{Bj}))/(1+r(x_{Bj}))$ in individual x_{Bj} bins at fixed Q^2. In order to do so we must employ a determination of $F_2^d(x_{Bj})$ which is not currently available from E665. There are some alternatives [36, 40] each of which is limited by the fact that, as yet, $F_2^d(x_{Bj})$ is not well constrained in this kinematic region. We have at this juncture chosen to use precisely the parameterisation given by NMC [36]. The evaluation of the sum rule requires that Q^2 be fixed, and we have chosen 4 GeV^2 which is within the range of our data for most values of x_{Bj}. This is also the value used by NMC. We have assumed that $r(x_{Bj})$ can be different bin by bin in x_{Bj}, constrained only by the individual measurements, this is a conservative assumption, the behaviour of $r(x_{BJ})$ is likely to be somewhat smooth.

Without taking into account the possible systematic errors discussed earlier we give as our result

$$\int_{0.001}^{0.125}(F_2^p - F_2^n)\frac{dx_{Bj}}{x_{Bj}} = -0.10 \pm 0.07.$$

At this stage the result is to be taken as preliminary, a publication with more detail is in preparation [41]. This result is consistent with the contribution to the integral found by NMC [36] in the region $0.004 < x_{Bj} < 0.15$ of 0.091 ± 0.007 (stat). Alternatively the result may be compared to 0.194 ± 0.004(stat)

which would be the contribution needed from this region to satisfy the Gottfried Sum Rule if the NMC data are correct at higher x_{Bj} but underestimate the contribution to the integral in this low x_{Bj} region. Our measurement indicates that this is unlikely.

Forward Hadron Fragmentation

The final state in muon scattering is dominated by light quarks, the charm and bottom quark content is small. Muon scattering thus provides a clean insight into light quark fragmentation and Quantum Chromodynamic (QCD) effects. In studying fragmentation we use the variables z_h and p_T; $z_h \equiv E_h/\nu$ is the fraction of the exchanged energy carried by the hadron, and p_T is the hadron transverse momentum, defined with respect to the direction of the exchanged virtual photon. The results [23] presented here are based on the charged hadrons, produced in the forward hemisphere of the total hadronic center of mass system, from a sample of ~11,000 muon–Deuterium scattering events. These events have survived cuts as follows: a minimum ν of 100 GeV, a maximum $y \leq 0.85$ ($y = \nu/E$), a lower limit of $Q^2 > 2$ GeV^2/c^2. The requirement on the hadronic energy fraction, $z_h > 0.1$, limited the sample of tracks to those which had adequate acceptance in the forward spectrometer.

Figure 9a shows the scaled energy distribution (z_h) for charged hadrons measured in this experiment. The average W^2 of the data set is 420 GeV^2. The error bars represent the statistical errors only. For comparison, data at somewhat lower W, measured by the EMC [42] and by earlier muon scattering experiments at Fermilab [43] are included. There are no obvious differences among the deep-inelastic muon scattering data sets. The data can be approximately represented by a simple exponential in z_h for $z_h > 0.1$. In Figure 9b the μd data are compared to those from e^+e^- annihilation at a comparable center of mass energy, taken from reference [44] and scaled by a factor 0.5 to ensure a comparison for one hemisphere only. In the interval $0.1 < z_h < 0.75$, the distribution measured in e^+e^- annihilation is slightly steeper. It has been suggested that this is due to the difference in the mix of quarks involved [42]. In Fig. 10 we show a comparison of our data with the fragmentation function measured [45] in $p\bar{p}$ interactions. Although the magnitude of the function at moderate z_h is comparable in the two interactions the $p\bar{p}$ data are much steeper. Within the QPM the fragmentation functions are postulated to be independent of the underlying hard scatter.

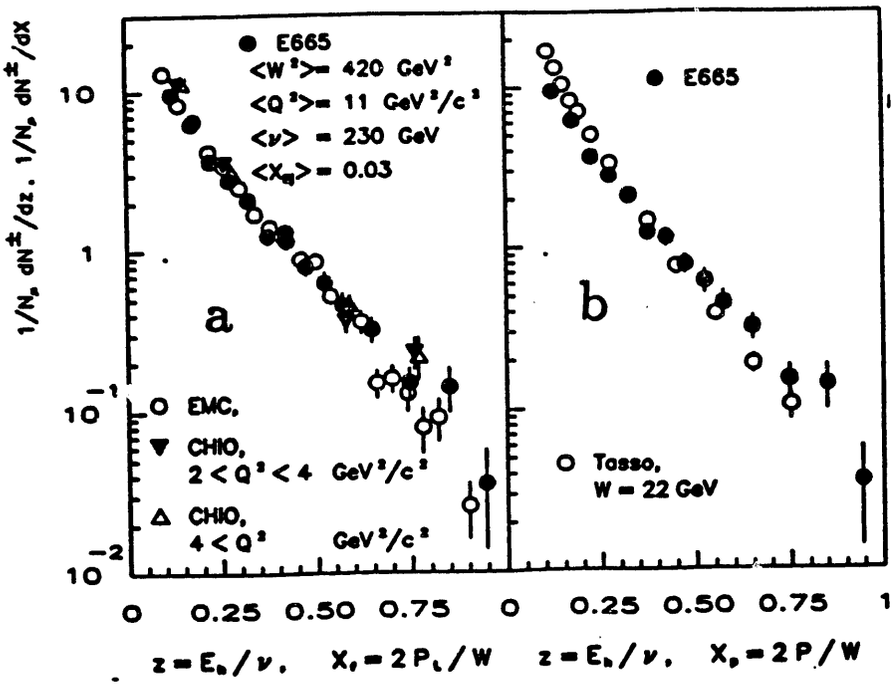

Figure 9

Forward fragmentation distributions compared to previous muon scattering experiments and to e^+e^- annihilation, z_h is used for the E665 results, x_f for the CHIO results and x_p for the Tasso results.

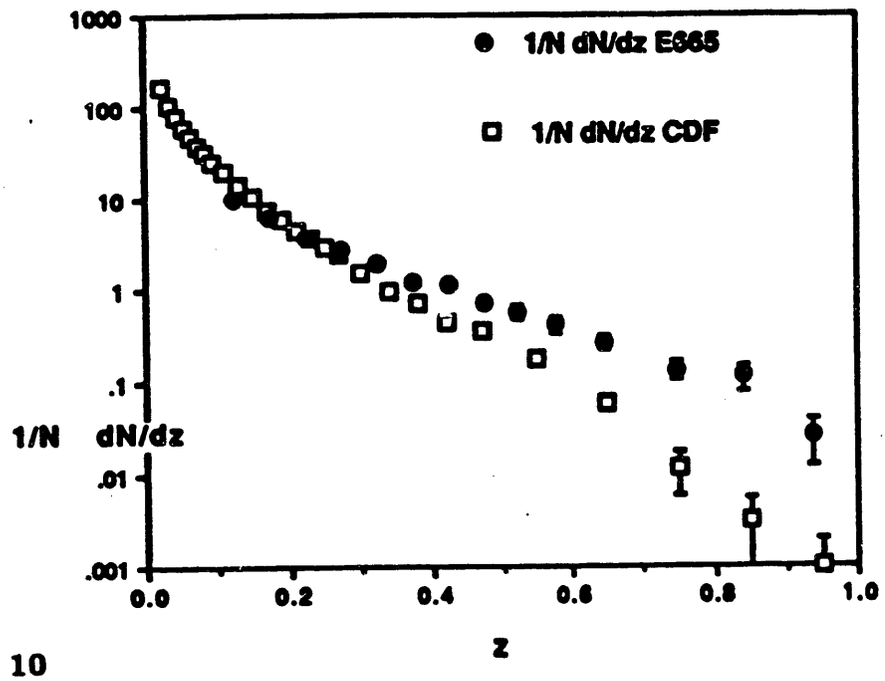

Figure 10

Comparison of fragmentation in muon scattering(E665) and $p\bar{p}$ annihilation (CDF).

A calculation based on QCD suggests deviations from this behavior leading to a steepening of the z_h distribution as W^2 increases[46]. Such steepening has been observed in muon scattering [47] and e^+e^- [48] interactions. In Fig. 11 we show the results of exponential fits to both the E665 and the TASSO [44] data.

In both data sets the slopes of the distributions become steeper as W^2 increases. Such a dependence would be expected as a result of QCD [46]; it is analogous to the QCD evolution of the structure functions. Given the comparison of Fig. 10, it seems that a combination of the data from these rather different reactions may give a coherent view of the scale breaking effects in fragmentation despite the differences in the identities of the fragmenting partons.

In Figure 12 we display the p_T^2 distributions, $(1/N_\mu)(dN^h/dp_T^2)$, measured in this experiment for three different ranges in W^2. The distribution at low p_T^2 show the typical steep decrease but are much flatter at high p_T^2. This is consistent with descriptions of such QCD processes as gluon bremsstrahlung. This feature is most evident for the highest W^2 data. Also in Fig. 12, some data from a recent EMC analysis are included, which used a merged data set of μp and μd interactions [49].

The average p_T^2 in lepton scattering has been heuristically described in terms of the contributions from three sources: the intrinsic momentum of the quarks in the nucleon, the p_T introduced by the fragmentation process, and the p_T introduced by perturbative QCD processes which may originate from either gluon emission by the participant quark or the photon gluon fusion mechanism. The intrinsic quark momentum should lead to an increase of the $\langle p_T^2 \rangle$ with z_h, as the hadron takes a fraction z_h of the initial quark transverse momentum. The fragmentation p_T up to rather high z_h is expected to be approximately constant in most models. The QCD contribution was predicted to grow proportionally to W^2 [50], as the phase space available for gluon emission grows. In Figure 13, we plot the average p_T^2 versus W^2 for three different z_h ranges: $0.1 < z_h < 0.2$ (a), $0.2 < z_h < 0.4$ (b), and $0.4 < z_h < 1.0$ (c). We have also included measurements [49, 51, 52, 53] from lower energy lepton scattering experiments. The expected behavior is evident; there is an increase of $\langle p_T^2 \rangle$ with W^2 as well as with z_h, and the higher energy data from this experiment connect smoothly to the lower energy data. The rise as a function of W^2 appears to weaken at higher W^2. Conceivably this is because the higher W^2 data tend to be at lower x_{Bj}.

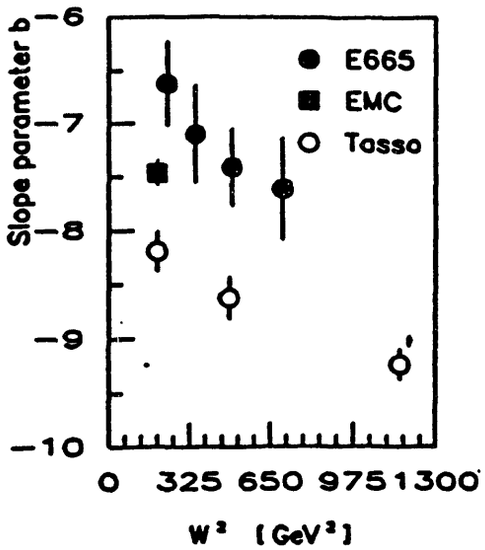

Figure 11

Slope of fragmentation function versus centre of mass energy squared, the slope parameter b, the result of a fit of a simple exponential to the fragmentation function is plotted as a function of W^2.

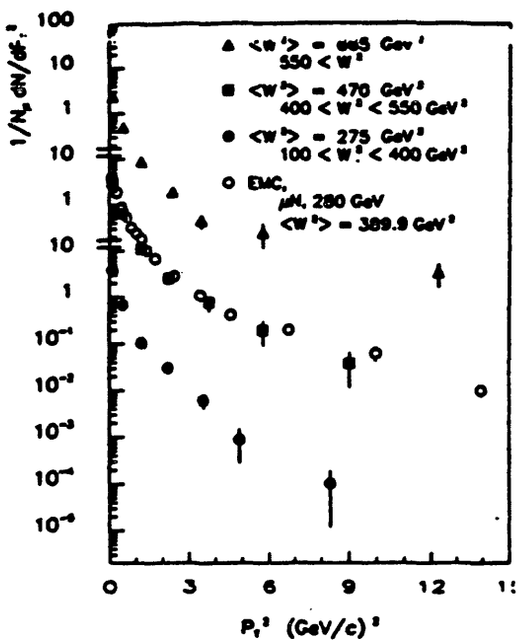

Figure 12

Transverse momentum distributions in muon scattering.

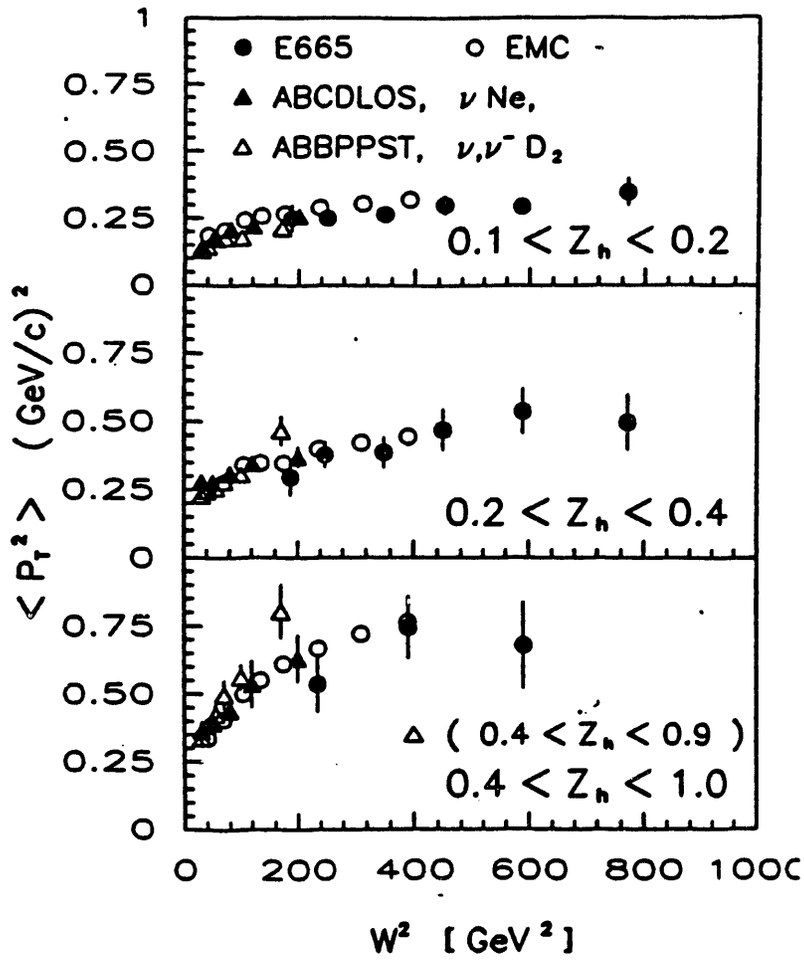

Figure 13

Average transverse momentum squared as a function of hadronic centre of mass energy squared in leptoproduction, data from E665 [23], EMC [49], Deden et al. [51] and Berggren et al. [53].

Forward Di-jet Production Rates

The distributions and data presented in the previous section are representative of the initial steps towards investigating the hadronic final state in leptoproduction in order to learn more about QCD. There have also been studies from this experiment [19] which have attempted analyses of the shapes of the final hadronic system. In this section we discuss the next step, an attempt to quantify these effects.

QCD corrections to the parton model predict, through photon-gluon fusion ($q\bar{q}$) and gluon bremsstrahlung (qg), di-jet production in the forward direction [50]. The cross sections for the production of $q\bar{q}$ and qg events have been calculated to first order in α_s [54]. To regulate collinear and soft singularities an invariant mass cut is usually introduced in these calculations. This cut is equivalent to a definition of the resolvability of the parton pairs. In contrast to e^+e^- jet production, the quark densities, as well as the fragmentation functions are involved in the deep inelastic jet cross-section calculations. In addition, DIS di-jet production depends on the gluon density inside the hadron target through the $q\bar{q}$ process. The results of a representative calculation are shown in Fig. 14.

The data sample of 17000 Hydrogen target events used for this analysis were subjected to the following kinematic cuts: $Q^2 > 2.5\ GeV^2$; $\nu \geq 40$ GeV; $x_{Bj} > 0.003$ and $0.05 \leq y_{Bj} \leq 0.95$. A further cut was used to remove the contribution of photon bremsstrahlung: events with $\nu > 200$ GeV, $E_{calorimeter}/\nu > 0.35$ and no charged hadron tracks were considered to be bremsstrahlung. Both charged particles reconstructed in the tracking system and fitted to the vertex and all neutral particles reconstructed in the calorimeter were used. The particles, both neutral and charged were transformed to the centre of mass of the hadronic system, for the charged hadrons the pion mass was assumed. The Jade [55] jet finding algorithm has been used to define the number of jets in an event. The "squared invariant mass" of a hadron pair, scaled by the squared total c.m.s visible energy in the event (E^2_{vis}) was used by the algorithm. A reasonable acceptance measured in terms of E_{vis} is not reached until W=15 GeV (70%), therefore only events with $W \geq 15$ GeV were used.

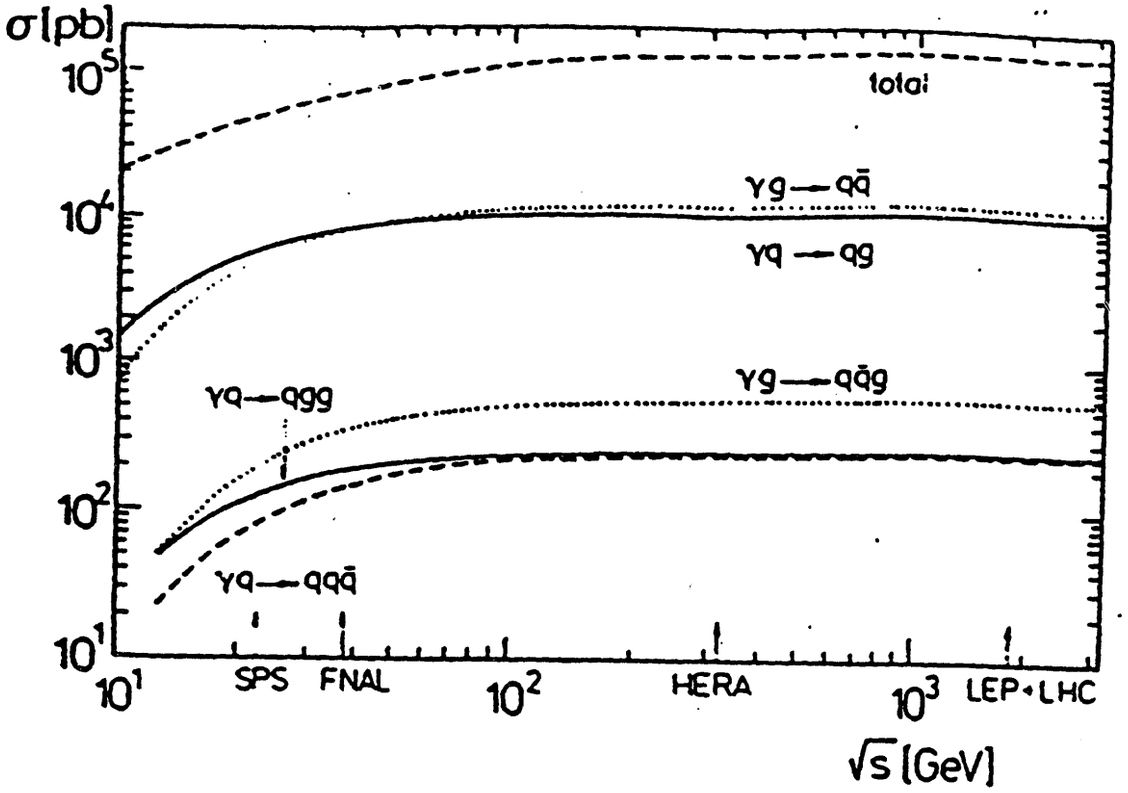

Figure 14
Predictions for yields of multi-parton final states.

Figure 15 shows the rates of one, two and more than two forward jets versus the resolution parameter in the algorithm, y_{cut}. The data have not been corrected for acceptance. The rates measured for di-jet production are comparable to those predicted. A detailed comparison formally requires correction of the data for acceptance and radiative effects. Further some understanding of the role of fragmentation in these distributions is needed. This approach may represent a first step towards a quantitative understanding the relative contributions of the different topologies, often identified with the different QCD terms, in deep inelastic scattering.

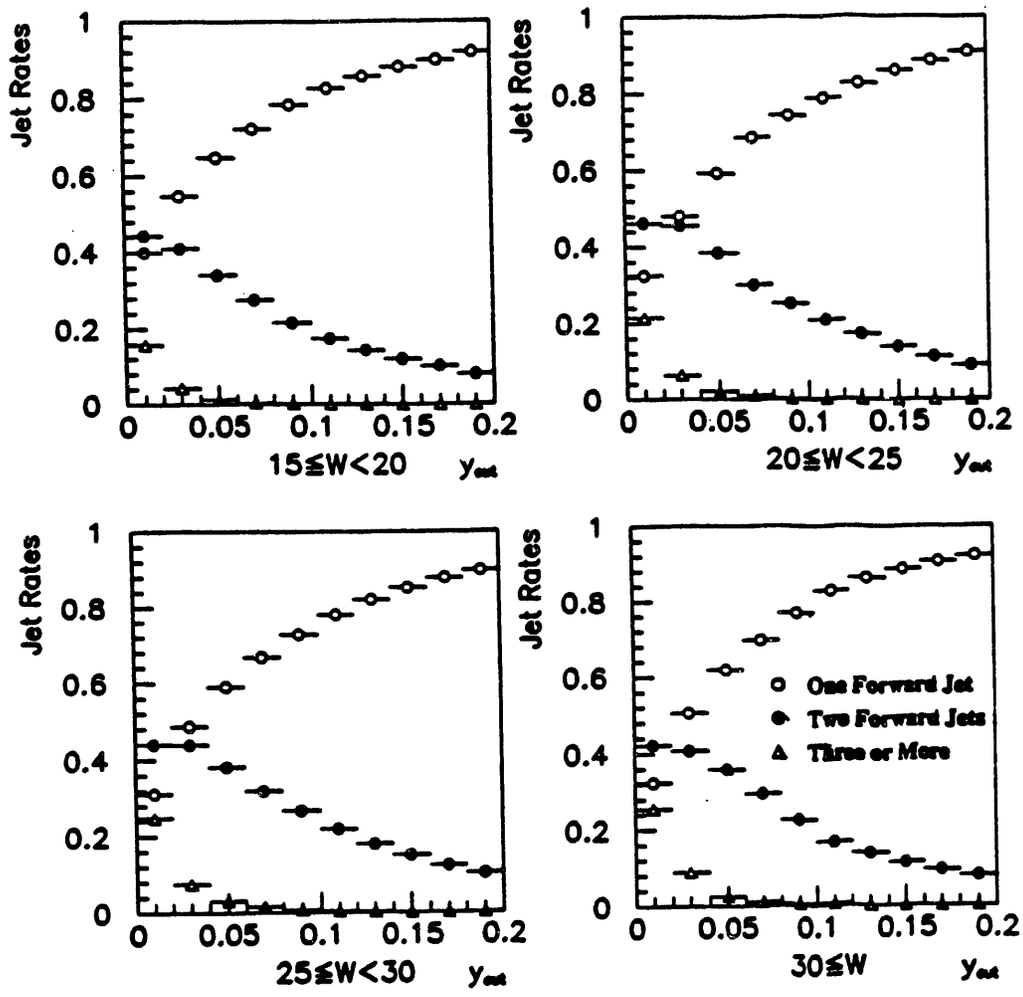

Figure 15

Jet fractions measured as a function of the y_{cut} parameter, for different centre of mass energy squared.

Conclusions

We have presented and discussed measurements of the ratio of deep inelastic scattering cross-sections from Xenon and Deuterium. These data extend the x_{Bj} range of available measurements and show clearly a flattening of the ratio as x_{Bj} gets smaller. The neutron to proton ratio data indicate that the solution to the puzzle of the non-saturation of the Gottfried Sum Rule does not lie in the range $0.001 \leq x_{Bj} \leq 0.1$. Fragmentation functions and their scale breaking show a remarkable consistency across μp, e^+e^- and $p\overline{p}$ interactions. Finally, rates for forward di-jet production have been measured.

The work of the University of California, San Diego was supported in part by the National Science Foundation, contract numbers PHY82-05900, PHY85-11584 and PHY88-10221; the University of Illinois at Chicago by NSF contract PHY88-11164; and the University of Washington by NSF contract numbers PHY83-13347 and PHY86-13003. The University of Washington was also supported by the U. S. Department of Energy. The work of Argonne National Laboratory was supported by the Department of Energy, Nuclear Physics Division, under Contract No. W-31-109-ENGGG-38. The Department of Energy, High Energy Physics Division, supported the work of Harvard University, the Unversity of Maryland, the Massachussetts Institute of Technology under Contract No. DE-AC02-76ER03069 and Yale University. The Albert-Ludwigs-Universität and the University of Wuppertal were supported in part by the Bundesministerium für Forschung and Technologie.

[a] Current address: Lawrence Livermore National Laboratory, Livermore, CA 94550, USA.

[b] Current address: The Rockefeller University, New York NY 10021, USA.

[c] Current address: Loma Linda University Medical Center, Loma Linda CA 92350 USA.

[d] Current address: Rutgers University, Piscataway, NJ 08855, USA.

[e] Current address: LeCroy Research Systems, Spring Valley, NY 10977, USA.

[f] Current address: DESY, Notkestr.85,2000 Hamburg, Germany.

[g] Current address: Argonne National Laboratory, Argonne, IL 60439, USA.

[h] Current address: California Institute of Technology, Pasadena, CA 91125, USA.

[i] Current address: Oxford University, Oxford, UK.

[j] Current address: Fermi National Accelerator Laboratory, Batavia, IL 60510, USA.

[k] Current Address A. T. & T, Bell Labs. 2000 North Naperville Road, Naperville, IL, USA.

[l] Deceased.

[m] Current address: Northern Illinois University, Dekalb, IL 60115, USA.

References

[1] S. Aid, Ph.D. Thesis, Univ. Maryland, September 1991.

[2] P.L.Anthony, Ph.D. Thesis, Massachusetts Institute of Technology, September 1990.

[3] A.A.Bhatti, Ph.D. Thesis, Univ. Washington, June, 1991.

[4] Uwe Ecker, Ph.D. Thesis, Univ. Wuppertal, February, 1991.

[5] Martin Erdmann, Ph.D. Thesis, Univ. Freiburg, March 1990.

[6] Douglas M. Jansen, Ph.D. Thesis, Univ. Washington, March 1991.

[7] Stephen Magill, Ph.D. Thesis, Univ. Illinois at Chicago, September, 1990.

[8] Douglas Grant Michael, Ph.D. Thesis, Harvard Univ. April 1990.

[9] Stephen Charles O'Day, Ph.D. Thesis, Univ. Maryland, September 1990.

[10] Eric J. Ramberg, Ph.D. Thesis, Univ. Maryland, September 1989.

[11] Arnd Roser, Ph.D. Thesis, Univ. Wuppertal, January 1991.

[12] John James Ryan, Ph.D. Thesis, Massachusetts Institute of Technology, December 1990.

[13] Alexander Salvarani, Ph.D. Thesis, Univ. California San Diego, February 1991.

[14] E665,S.Wolbers, FERMILAB-Conf-88/153-E, August, 1988, Presented at the Meeting of the Division of Particles and Fields of the APS, Storrs, CT, 1988.

[15] E665,S.Magill, FERMILAB-Conf-90/127-E, 1990, Presented at the Meeting of the Division of Particles and Fields of the APS, Houston, Texas, 1990.

[16] E665, M.Schmitt, FERMILAB-Conf-90/126-E, August, 1990, Presented at the XXVth Rencontres de Moriond: High Energy Hadron Interactions, Les Arcs, France, 1990.

[17] E665, S. Aid, Workshop on Hadron Structure Functions and Parton Distributions, Fermilab, April 1990, Ed D.F.Geesaman, J.Morfin, C.Sazama and W.K.Tung, World Scientific, 1990.

[18] E665, M.R.Adams et al., Xe/D Paper submitted to the XXVth Int. Conf. on High Energy Physics, Singapore, 1990. E665, C.Halliwell, Paper presented to the XXVth Int. Conf. on High Energy Physics, Singapore, 1990.

[19] E665, M.R.Adams et al., Paper submitted to the XXVth Int. Conf. on High Energy Physics, Singapore, 1990. E665, H.Lubatti, FERMILAB-Conf-90/271-E(1990), Paper presented to the XXVth Int. Conf. on High Energy Physics, Singapore, 1990.

[20] E665, M.R.Adams et al., Paper submitted to the XXVth Int. Conf. on High Energy Physics, Singapore, 1990.

[21] E665, S. Wolbers, FERMILAB-Conf-90/233-E, 1990, Presented at the XX International Symposium on Multiparticle Dynamics, Gut Holmecke, Germany, September, 1990.

[22] E665, D.Jaffe, Presented at the XXVIth Rencontres de Moriond, Les Arcs, France, 1991.

[23] E665, M.R.Adams et al., Fermilab-Pub-91/217,August, 1991.To be Published in Physics Letters.

[24] E665, C.Salgado, Fermilab-Conf-91/225-E, Presented at the Meeting of the Division of Particles and Fields of the APS, Vancouver,Canada, 1991.

[25] A. Malensek and J.G.Morfin FERMILAB TM-1193 (1983).

[26] E665, M.R. Adams et al., Nucl. Inst. and Meth. **A291** (1990) 533.

[27] NMC, P.Amaudruz et al., CERN/PPE-91-52(1991) submitted to Z. Phys.

[28] J.Kuti and V.Weisskopf, Phys. Rev. D4 (1971) 3418.

[29] K.Gottfried, Phys. Rev. Lett. 18 (1967) 1174.

[30] R.Field and R.P.Feynman, Phys. Rev. D15 (1977) 2590.

[31] A.Bodek et al., Phys. Rev. D20 (1979) 1471.

[32] CHIO,B.A.Gordon et al., Phys Rev D20, 2645 (1979).

[33] EMC,J.J.Aubert et al., Nucl. Phys. B293, 740 (1987).

[34] BCDMS,A.C.Benvenuti et al., Phys. Lett. 237B, 599 (1989).

[35] NMC,D. Allasia et al., Phys. Lett. 249B, 366 (1990).

[36] NMC,P.Amaudruz et al., Phys. Rev. Lett. 66 (1991) 2712.

[37] A.D.Martin, W.J.Stirling and R.G.Roberts, Durham U. Preprint, DTP/90/62, Rutherford Preprint, RAL-90-068, 1990.

[38] G.Preparata, P.G.Ratcliffe and J.Soffer, Marseilles Preprint, MITH 90/11, 1990.

[39] L.Whitlow, Ph. D. Thesis, SLAC-357, 1990.

[40] J.G. Morfin and Wu-Ki Tung, FERMILAB-Pub-90/74; April, 1990.

[41] M.R.Adams et al., Publication in Preparation.

[42] M.Arneodo et al., Z. Phys. C - Particles and Fields **35** (1987) 417.

[43] W.A.Loomis et al., Phys. Rev. D19 (1979) 2543.

[44] M.Althoff et al., Z. Phys. C - Particles and Fields **22** (1984) 307, (Table 4f and Figure 40).

[45] F.Abe et al., Phys. Rev. Lett. **65** (1990) 968.

[46] R.Baier, K.Fey, Z. Physik C, Particles and Fields **2** (1979) 339.

[47] M.Arneodo et al., Phys. Lett. **165B** (1985) 222;
J.J.Aubert et al., Phys. Lett. **114B** (1982) 373.

[48] D.H.Saxon, *Quark and Gluon Fragmentation in High Energy e^+e^--Annihilation,* Rutherford Appleton Laboratory, RAL–86–057, July 1986.

[49] J.Ashman et al., CERN-PPE-53(1991) to be submitted to Zeitschrift für Physik.

[50] G.Altarelli, G.Martinelli, Phys. Lett. **76B** (1978) 89.

[51] H.Deden et al., Nucl. Phys. **B181** (1981) 375.

[52] D.Allasia et al., Z. Phys. C27, 239 (1985).

[53] M.Berggren et al., Z. Phys. C50, 427 (1991).

[54] J.G.Korner,E.Mirkes,G.Schuler;*Int.J.Mod.Phys.* **A4** (1989) 1781.

[55] JADE,W.Bartel et al., Z. Phys **C33**(1986) 23.

END

DATE FILMED

12/17/91